Analysis and simulation of a three-phase push-pull/flyback interleaved bidirectional dc-dc converter

Menaouar Berrehil El Kattel[1]. Robson Mayer[1]. Sérgio Vidal Garcia Oliveira[1,2].
[1] Santa Catarina State University UDESC, Joinville - Santa Catarina - Brasil
[2] Blumenau Regional University FURB, Blumenau - Santa Catarina - Brasil
E-mail: berrehilelkattel@gmail.com, mayerrobson@gmail.com, sergio_vidal@ieee.org

***Abstract*— This paper presents a new bidirectional dc/dc converter topology, which is composed of three-phase push-pull and interleaved flyback converter. The two directions operation of the proposed converters is analyzed and explained even as the DC transfer function of the circuit versus the duty ratio has been presented. The main advantages of this topology are high switching frequency, lower input current ripple, smaller output capacitor, less number of switches and the frequency of output voltage and input current ripple are three times the switching frequency. A simulation model is developed in the OrCAD Capture simulator. Then, the simulation results will verify the validity of the mathematical and theoretical analysis.**

***Keywords* - Interleaved flyback converter, Push-pull converter, Three-phase dc-dc converter, Bidirectional, Isolated.**

I. INTRODUCTION

The power processing needs every day more electronic devices of high capacity and reliability, such as dc-dc converters to control the system power flow. Applications including energy storage systems, solid-state transformers, distributed generation, uninterruptible power supplies, fuel cell, transportation, and electric vehicles. The application of high-frequency three-phase or multi-phase converters enables magnetic elements, such as the transformer, work more efficiently, increases power density, reducing the current stress on the power semiconductors and reducing the ripple voltage on the filter capacitor, allows applying high turns ratio for high gain and provides galvanic isolation between the power source and load [1].

In particular, the high-frequency three-phase dc–dc converter has two major advantages over its single-phase counterpart. That are, the reduction of the input and output filters' volume due to increased effective switching frequency and reduction in transformer size and volume compared with a three equivalent single-phase transformers. Furthermore, the dc-dc converter needs to have bidirectional power flow capability when energy storage is needed in the system [2-3]. Several different types of bidirectional dc–dc converters with high-frequency three-phase transformer have been published in the literature [4-6]. A three-phase converter has basically voltage-fed nature's on both ports where the source and load are connected [7-13], but current-fed converter has been developed for use in low voltage sources [14-17]. Most of them require more components and complex control techniques. Another structure to increase power density and reduce control complexity is based on flyback converters [18], [19], and interleaved multiphase converters have been used [20–22].

Renewable energies such as photovoltaic, wind energy, bioenergy, and fuel cells, are becoming increasingly important and widely used in distribution systems or in microgrids. Microgrid systems has been receiving more attention from industry and researchers to facilitate the integration of these different sources of energy generation. It allows power generation near the consumer loads, which reduces costs and losses on the transmission lines. To control the power flow between the different sources, loads, and energy storage, the dc-dc converters are needed, and current-fed converters have a smaller energy storage devices, and for microgrid application, that offer high step-up/step-down ratio.

II. PROPOSED BIDIRECTIONAL DC-DC CONVERTER

Fig. 1 shows the circuit topology of the three-phase push-pull/flyback interleaved bidirectional converter. In direction A to B it operates as a three-phase push-pull converter for converting power from low to high voltage and in direction B to A as three-phase interleaved flyback converter for converting power from high to low voltage. In direction A to B, the converter consists of a three-phase dc-dc converter, which output is connected to a three-phase full-bridge diode rectifier through three-phase transformer, three main switches (S_1, S_2, S_3), three coupled inductors (T_{F1}, T_{F2}, T_{F3}), diodes (D_7, D_8, D_9, D_{S4}, D_{S5}, D_{S6}), an energy store capacitor C_1, input DC voltage E_1 and output DC voltage E_2. In direction B to A, the converter is composed by the input DC voltage E_2, the output DC voltage E_1, the switches (S_4, S_5, S_6), the diodes (D_{10}, D_{11}, D_{12}), the output capacitor C_2 and the coupled inductors (T_{F1}, T_{F2} and T_{F3}).

The analysis of proposed converter in direction A to B is similar to converters mentioned in [23-24], where the circuit has three duty ratio intervals for switching period.

The circuit in the direction B to A is very similar to interleaved flyback topologies [25-26]. For the operation in this direction, a duty ratio varies from 0 to 1/3, where the switches operate in the nonoverlapping conduction mode.

The following sections will describe the operating principles and steady-state analysis for both directions.

Figure 1. Proposed three-phase push-pull/flyback interleaved bidirectional converter

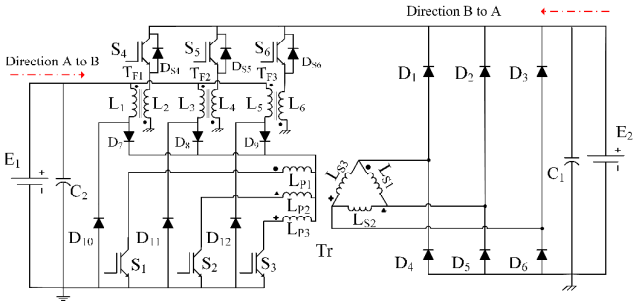

III. OPERATION PRINCIPLE OF THE PROPOSED CONVERTER

In this section, the operational analysis is presented considering all the circuit components are assumed to be ideal. The proposed converter can operate in two sides. Based on Fig. 1, these sides are denoted by direction A-to-B and direction B-to-A.

A. *Operational principle in direction A-to-B*

The proposed structure presents different stages in continuous operation mode (CCM) with a duty ratio (D) lower than 1/3, between 1/3 ≤ D ≤ 2/3 and higher than 2/3. The following sections are described the more detailed stages analysis in CCM.

1) Operation in the duty ratio range 0 < D < 1/3

In the 1st, 3rd, and 5th stages, the power source provides energy to the load, and part of this energy is stored in the windings L_1, L_3 e L_5. In the 2sd, 4th, and 6th stages, the energy stored in L_1, L_3 e L_5 is discharged to the load by the internal diode of switches S_4, S_5 and S_6. Analysis of the 1st and 2sd stages are acceptable to present the operational stages of the proposed topology.

a) 1st Stage [($t_0 \rightarrow t_1$) Figure 2(a)]: The power switch S_1 is conducting at t = t_0. The input inductors L_1, L_3 and L_5 store energy from power source E_1 and input current $i_{E1}(t)$ increases linearly. The voltage across L_1 and L_{p1} are, respectively, equal to the E_1-(E_2/n_T) e E_2/n_T.

$$v_{L1}(t) = E_1 - E_2 / n_T \qquad v_{Lp1}(t) = E_2 / n_T$$
$$i_{E1}(t) = 3i_{L1}(t) = i_{S1}(t) \qquad \Delta t_1 = t_1 - t_0 = D\,T_S \tag{1}$$

b) 2nd Stage [($t_1 \rightarrow t_2$) Figure 2(b)]: At the instant t = t_1, power switch S_1 is turned-off and current $i_{E1}(t)$ decreases linearly. The energy stored in the primary windings L_1, L_3 and L_5 is delivered to the load through the secondary windings L_2, L_4, L_6 and the internal diode of switches S_4, S_5 and S_6. The voltage across L_1 is equal to the E_2/n_S.

$$v_{L1}(t) = -E_2 / n_S \qquad v_{Lp1}(t) = -E_2 / n_T$$
$$i_{E1}(t) = 0 \qquad \Delta t_2 = t_1 - t_2 = \frac{1-3D}{3} T_S \tag{2}$$

2) Operation in the duty ratio range 1/3 ≤ D ≤ 2/3

a) 1st Stage [($t_0 \rightarrow t_1$) Figure 2(c)]: At the moment t = t_0, the power switches S_1 e S_3 are turned-on. The windings L_1, L_3 e L_5 store energy from E_1 and current $i_{E1}(t)$ increases linearly. The load receives energy from E_1 by windings L_{S1}, L_{S3}, diode D_2 and D_6. The equations of the input current $i_{E1}(t)$, $v_{L1}(t)$, $v_{Lp1}(t)$, and the interval of this stage are described as the following.

$$v_{L1}(t) = E_1 - (2E_2 / n_T) \qquad v_{Lp1}(t) = E_2 / 2n_T$$
$$i_{E1}(t) = 3i_{L1}(t) = 2i_{S1}(t) \qquad \Delta t_1 = \frac{3D-1}{3} T_S \tag{3}$$

b) 2sd Stage [($t_1 \rightarrow t_2$) Figure 2(d)]: Starts when power switch S_3 is turned-off. The windings L_1, L_3 e L_5 are demagnetized and input current $i_{E1}(t)$ decreases linearly. The load receives energy from the power source E_1 through winding L_{S1}, diodes D_2, and D_4. The expressions of the input current $i_{E1}(t)$, $v_{L1}(t)$, $v_{Lp1}(t)$, and the interval time of this stage are described as the following.

$$v_{L1}(t) = E_1 - (E_2 / n_T) \qquad v_{Lp1}(t) = E_2 / n_T$$
$$i_{E1}(t) = 3i_{L1}(t) = i_{S1}(t) \qquad \Delta t_2 = \frac{2-3D}{3} T_S \tag{4}$$

The analysis of 3rd and 5th stages are similar to the 1st stage, and the analysis of 4th and 6th stages are similar to the 2nd stage. The difference between each other is the modulation of the switches. After the 6th stage a switching period is ended.

3) Operation in the duty ratio range 2/3 ≤ D ≤ 1

a) 1st Stage [($t_0 \rightarrow t_1$) Figure 2(e)]: At = t_0, power switches S_1, S_2 and S_3 are conducting. The windings L_1, L_3 and L_5 store energy from input E_1 and input current $i_{E1}(t)$ begins to increase linearly. The diodes of the rectifier bridge are reverse-biased and the output capacitor C_1 is discharged to supply the load. The circuit equations can be expressed as:

$$v_{L1}(t) = E_1 \qquad v_{Lp1}(t) = 0$$
$$i_{E1}(t) = 3i_{L1}(t) = 3i_{S1}(t) \qquad \Delta t_1 = \frac{3D-2}{3} T_S \tag{5}$$

b) 2sd Stage [($t_1 \rightarrow t_2$) Figure 2(f)]: At t = t_1, power switches S_1 and S_3 continue conducted and S_2 is turned-off. Windings L_1, L_3 and L_5 begin release the stored energy and input current $i_{E1}(t)$ starts to decrease linearly. The load will be powered from the power source E_1 through windings L_{S1}, L_{S3}, diodes D_2 and D_6. The circuit equations can be given by (6).

$$v_{L1}(t) = E_1 - (E_2 / 2n_T) \qquad v_{Lp1}(t) = E_2 / 2n_T$$
$$i_{E1}(t) = 3i_{L1}(t) = 2i_{S1}(t) \qquad \Delta t_2 = (1-D)\,T_S \tag{6}$$

The 3td and 5th stages are similar to the 1st stage and the 4th and 6th stages are similar to the 2nd stage. The difference between each other is the modulation of the switches. At the end of the sixth stage, the operating period of the proposed converter in CCM is completed.

B. *Operational principle in direction B-to-A*

a) 1st Stage [($t_0 \rightarrow t_1$) Figure 3(a)]: At the moment t = t_0, power switch S_4 is conducting and the diodes D_{11} and D_{12} are forward-biased. Windings L_2 stores energy from power source E_2 and the energy stored in windings L_4 and L_6 is transferred to the load through windings L_3, L_5, diodes D_{11} and D_{12}. The voltage and current across inductance L_2 and interval time can be displayed as following equation:

$$v_{L2}(t) = E_2 \qquad i_{E2}(t) = i_{L2}(t)$$
$$\Delta t_1 = D\,T_S \tag{7}$$

b) 2sd Stage [($t_1 \rightarrow t_2$) Figure 3(b)]: At t = t_1, S_4 is turned-off and the diode D_{10} is forward-biased. Inductors L_1, L_3 and L_5 transfer energy to the load through D_{10}, D_{11} and D_{12}, and no energy is transferred from the power source. One can derive the equation (8)

$$v_{L2}(t) = E_1 / n_S^{'} \qquad i_{E2}(t) = 0$$
$$\Delta t_2 = \frac{1-3D}{3} T_S \tag{8}$$

c) 3td stages [($t_2 \rightarrow t_3$) Figure 3(c)]: At instant t_2, power switch S_5 is turned-on and the diode D_{11} is reverse-biased. The winding L_4 stores energy by the power source E_2. Windings L_1 and L_5 continue transferred energy to the load through diodes D_{10} and D_{12}. The voltage and current across L_4 and time interval can be expressed via (9) as:

$$v_{L4}(t) = E_2 \qquad i_{E2}(t) = i_{L4}(t)$$
$$\Delta t_3 = D\,T_S \tag{9}$$

d) 5th Stage [($t_4 \rightarrow t_5$) Figure 3(d)]: At t = t_4, the power switch S_6 is conducting and D_{12} is reverse-biased. Winding L_6 stores energy from E_2; windings L_1 and L_3 continue transferred energy to the load through diodes D_{10} and D_{11}. The voltage and current across inductance L_6 and time interval can be denoted by equation (10).

$$v_{L6}(t) = E_2 \qquad i_{E2}(t) = i_{L6}(t)$$
$$\Delta t_5 = D\,T_S \tag{10}$$

The 4th and 6th stages are equal to the 2nd stage. After the 6th stage, the switching period is ended and it begins again with the 1st stage.

IV. Mathematical Analysis of Proposed Topology in CCM

In this section, the DC transfer function and input inductor value of proposed converter are presented in both directions.

A. DC transfer function

The expression DC transfer function in direction A to B, for CCM, can be described from the average voltage value across the winding L_1.

$$V_{L1} = \frac{3}{T_S}\int_0^{\Delta t_1} v_{L1}(t)\,dt + \int_0^{\Delta t_2} v_{L1}(t)\;dt = 0 \tag{11}$$

Substituting (1) and (2) into (11), (3) and (4) into (11) and finally (5) and (6) into (11), the value of DC transfer function in direction A to B can be derived by equation (12).

Where n_T turns ratio of three-phase transformers (Tr), n_S turns ratio of coupled inductors. D is the duty ratio of the switches S_1, S_2 and S_3. The turns ratio n_T and n_S are defined from equation (13).

Where n_{L1} and n_{L2} are the winding turns in the primary and secondary sides of the coupled inductor (T_{F1}~T_{F3}). n_{Lp1} and n_{Ls1} are the winding turns in the primary and secondary sides of the three-phase transformer (Tr.)

$$\frac{E_2}{E_1} = \begin{cases} \dfrac{3D \cdot n_S \cdot n_T}{3D(n_S - n_T) + n_T} & 0 < D < 1/3 \\ \dfrac{2\,n_T}{3(1-D)} & 1/3 \le D \le 2/3 \\ \dfrac{2\,n_T}{3(1-D)} & 2/3 \le D \le 1 \end{cases} \tag{12}$$

$$n_T = n_{Ls1} / n_{Lp1} \qquad n_S = n_{L2} / n_{L1} \tag{13}$$

DC transfer function for direction B to A in steady state can be determined from the average voltage of the inductor (L_2) for switching period (T_S). The discharge time of inductor L_2 is time interval, which corresponds to the (1-D) T_S, equation (14) indicates the average voltage across L_2.

$$V_{L2} = \frac{1}{T_S}\int_0^{DT_S} v_{L2}(t)\,dt + \int_0^{(1-D)T_S} v_{L2}(t)\;dt = 0 \tag{14}$$

During the magnetization and demagnetization of inductor L_2, its voltage is equal E_2 and E_1/n_S' respectively. Solving equation (15) leads to the DC transfer function for CCM operation for direction B to A.

$$\frac{E_1}{E_2} = \frac{D \cdot n_S^{'}}{(1-D)} \tag{15}$$

Where $n_S^{'}$ equal $1/n_S$ and D is the duty ratio of the switches S_4, S_5 and S_6.

The inductance value of L_1, L_3 and L_5 in direction A to B for CCM, can be obtained by equations (16)

$$L_{1.3.5} = \begin{cases} \dfrac{E_2 \cdot (1-3D)}{n_S \cdot f_S \cdot \Delta i_{E1}} & D < 1/3 \\ \dfrac{E_2 \cdot (2-3D) \cdot (3D-1)}{2n_T \cdot f_S \cdot \Delta i_{E1}} & 1/3 \le D \le 2/3 \\ \dfrac{3}{2}\dfrac{E_2 \cdot (1-D) \cdot (3D-2)}{n_T \cdot f_S \cdot \Delta i_{E1}} & 2/3 \le D \le 1 \end{cases} \tag{16}$$

Expression (17) can be used to determine the inductance value of winding L_2, L_4 and L_6 in direction B to A for CCM, which is valid within the range of duty ratio from 0 at 1/3.

$$L_{2.4.6} = \frac{E_1 \cdot (1-D)}{\Delta i_{E2} \cdot f_S \cdot n_S^{'}} \tag{17}$$

The expressions (12) of the DC transfer function of proposed converter operating in CCM for direction A to B is represented graphically in Fig. 4. It can be observed from Fig. 2 that the DC transfer function has the same feature of topologies cited in [27–28], when the duty ratio is higher than 2/3. For duty ratio less than 1/3, the proposed converter contains the DC transfer function of the isolated buck-boost dc-dc converter.

Fig. 5 shows the characteristics of the DC transfer function as functions of duty ratio (D) in CCM for direction B to A. It can be noted in this figure, with duty ratio less than 1/3, that the proposed topology operates as buck converter.

Figure 2. Equivalent circuit of stages for CCM in direction A to B

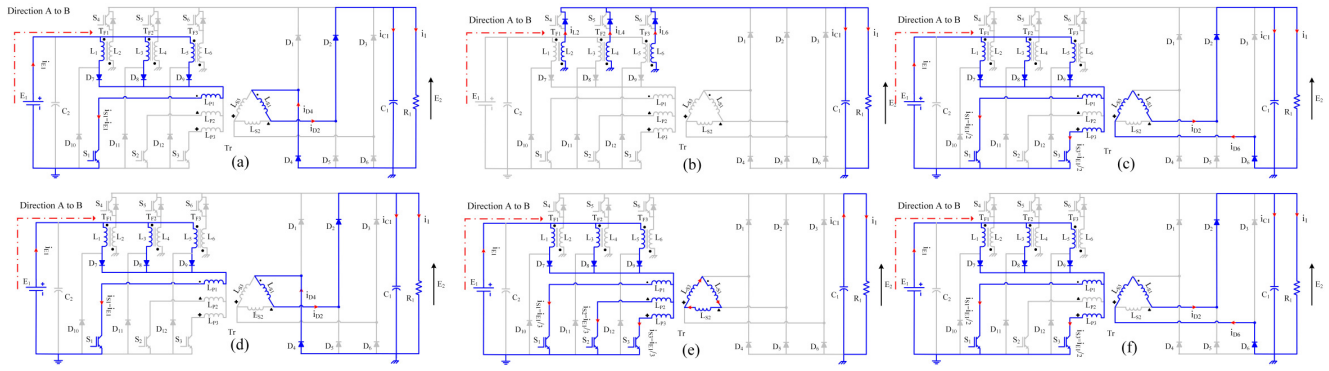

Figure 3. Equivalent circuit of stages for CCM in direction B to A

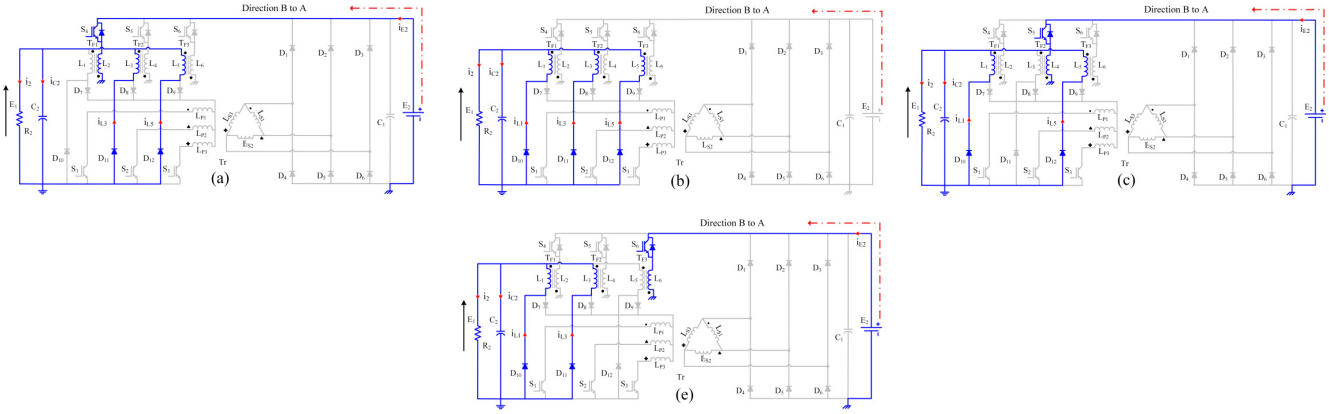

Figure 4. DC transfer function against duty ratio D

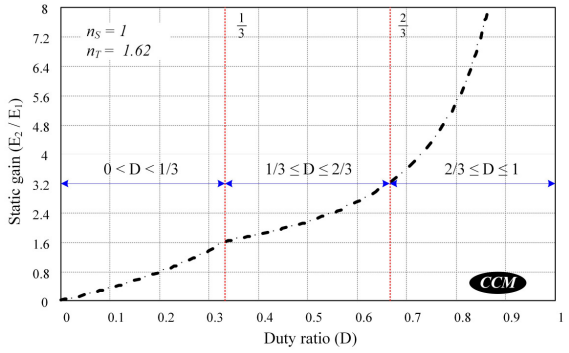

Figure 5. DC transfer function against duty ratio D

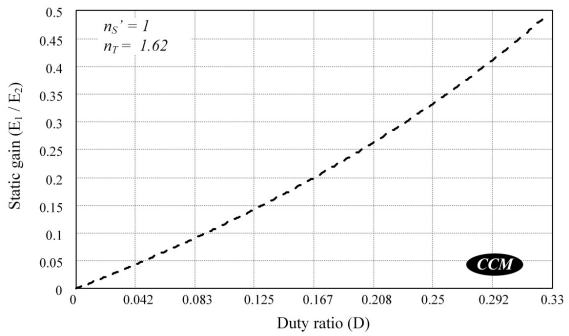

V. SIMULATION RESULTS

To verify the mathematical analysis and operational principles of proposed topology in CCM, a OrCAD simulation is conducted. The simulation parameters for operating in direction A to B and B to A are presented in Table I. All the components are assumed to be ideal. The simulation waveforms are presented below

TABLE I. CONVERTER SPECIFICATIONS

Description	Direction A to B	Direction B to A
Input voltage	150 V	540 V
Output voltage	540 V	150 V
Nominal power	3 kW	2 kW
Duty ratio	0.7	0.217
Switching frequency	40 kHz	40 kHz
Output voltage ripple	5 V	3V
Input current ripple	3.6 A	7.5A
Input inductance L_1	375 uH	
Ouput capacitor	926 nF	11.25 uF

A. *Simulation in direction A to B*

In Fig. 6, input and output current are shown as well as, the currents through coupled inductor L_1 and L_2. It can be noted that there is no current in the winding L_2 and the stored energy is delivered to the load through the winding L_1, these simulation results have similar trends to the theoretical operational analysis when the converter operates 2/3<D<1.

Additionally, the frequencies of output voltage and input current ripple is three times the switching frequency.

Figure 6. (a); output current i_{E2}, (b); inductor current i_{L1}, (c); inductor current i_{L2}, (d); input current i_{E1} for D = 0.7

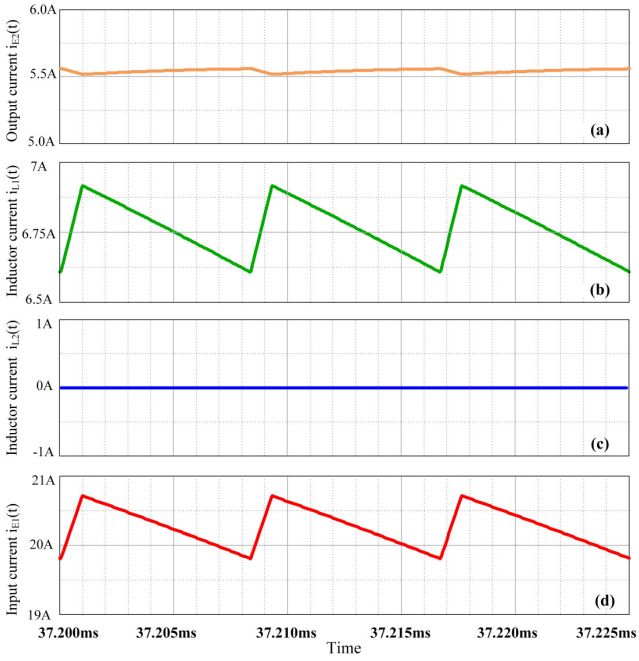

The input and output voltage waveforms are illustrated in Fig 7. The ripple present in output voltage waveforms are 5 V which confirms the specifications of converter.

Figure 7. Input and output voltage for D = 0.7

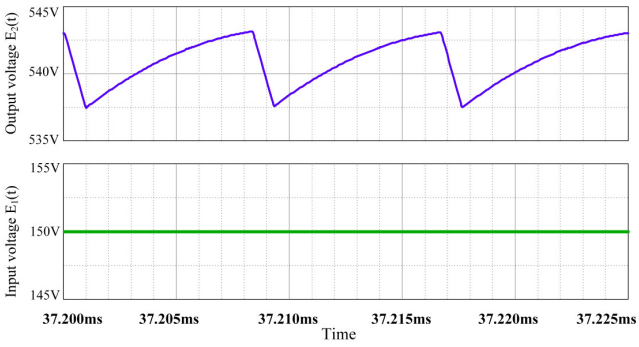

B. Simulation in direction B to A

In Fig. 8, the current across winding L_2 and L_1 are shown together with output and input current for direction B to A. It is observed that the stored energy in winding L_2 is delivered to the load by the winding L_1. Furthermore, the frequencies of output voltage and input current ripple is three times the switching frequency.

Fig 9 shows input and output voltage waveforms when operating in direction B to A. Window (a) and (b) refers E_1 (output voltage) and E_2 (input voltage) respectively. It is possible to observe that ripple output voltage is 3 V which confirms the specifications of converter.

Figure 8. (a); input current i_{E2}, (b); inductor current i_{L2}, (c); inductor current i_{L1}, (d); output current i_{E1} for D = 0.217

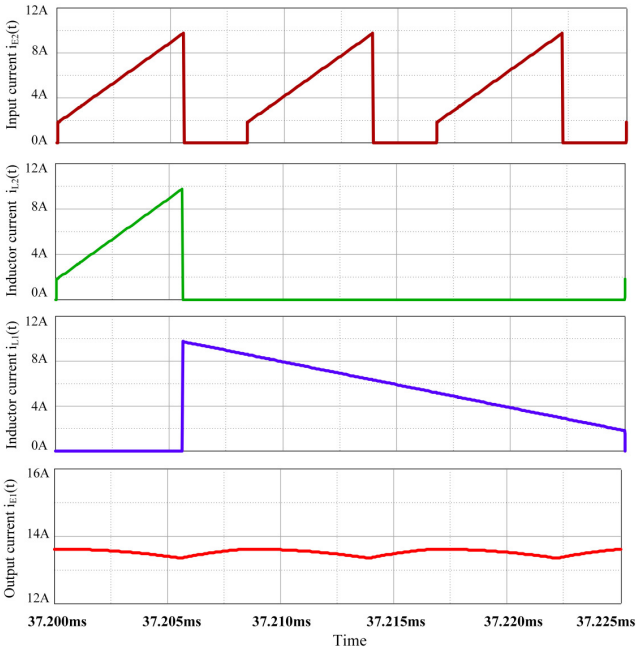

Figure 9. Input and output voltage for D = 0.217

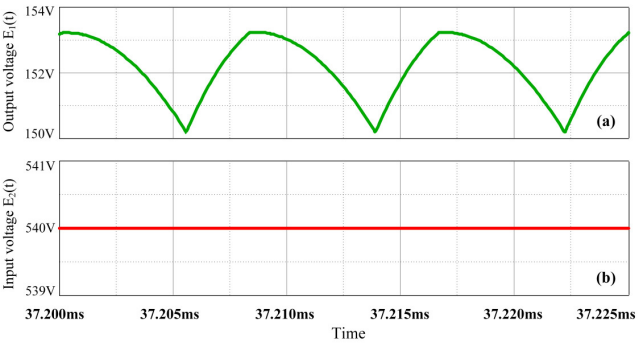

VI. CONCLUSION

In this paper, a novel three-phase current-fed push–pull/flyback interleaved bidirectional dc–dc converter has been proposed, designed and analyzed for high-power applications. The DC transfer function has been described for both of direction modes of operation. The simulation results have demonstrated that the capacitor size of the converter is reduced. Moreover, the current and voltage ripples are reduced by three times, and the converter seems to be very promising in high-power renewable energies or in microgrids systems applications.

ACKNOWLEDGMENT

The authors would like to thank to Coordination for the Improvement of Higher Education Personnel – CAPES, Technological Institute Foundation of Joinville – FITEJ and Foundation for Support of Scientific and Technological Research in the State of Santa Catarina – FAPESC for financial support.

REFERENCES

[1] A. R. Prasad, P. D. Ziogas, and S. Manias, "Analysis and design of a three-phase offline DC-DC converter with high frequency isolation," Industry Applications Society Annual Meeting, 1988., Conference Record of the 1988 IEEE, vol. 1, pp. 813–820, Oct. 1988

[2] G. Jia S., and L. Tang, "A Three-Phase Bidirectional DC-DC Converter for Automotive Applications," Industry Applications Society Annual Meeting, 2008. IAS '08. IEEE, pp. 1–7, Oct. 2008.

[3] P. C. Kjaer, S. Norrga, and S. Ostlund, "A primary-switched line-side converter using zero-voltage switching," IEEE Transactions on Industry Applications, vol. 37, no. 6, pp. 1824–1831, Nov. 2001.

[4] R. W. De Doncker, D. M. Divan, and M. H. Kheraluwala, "A three-phase soft-switched high power density DC/DC converter for high power applications," Industry Applications Society Annual Meeting, 1988., Conference Record of the 1988 IEEE, vol. 1, pp. 796–805, Oct. 1988.

[5] S. P. Engel, N. Soltau, and R. W. De Doncker, "Instantaneous current control for the three-phase dual-active bridge DC-DC converter," IEEE Energy Conversion Congress and Exposition (ECCE), pp. 3964–3969, 2012.

[6] N. Soltau, S. P. Engel, H. Stagge, and R. W. De Doncker, "Compensation of asymmetric transformers in high-power DC-DC converters," ECCE Asia Downunder (ECCE Asia), 2013 IEEE, pp. 1084–1090, June 2013.

[7] F. M. Ni, and T. L. Lee, "Implementation of a bidirectional three-phase dual-active-bridge DC converter for electric vehicle applications," Future Energy Electronics Conference (IFEEC), 2013 1st International, pp. 271–276, Nov. 2013.

[8] N. H. Baars, J. Everts, H. Huisman, J. L. Duarte, and E. A. Lomonova, "A 80-kW Isolated DC–DC Converter for Railway Applications," IEEE Transactions on Power Electronics, vol. 30, no. 12, pp. 6639–6647, Dec. 2015.

[9] N. Soltau, H. Stagge, R. W. De Doncker, and O. Apeldoorn, "Development and demonstration of a medium-voltage high-power dc-dc converter for dc distribution systems," IEEE 5th International Symposium on Power Electronics for Distributed Generation Systems (PEDG), pp. 1–8, June 2014.

[10] F. M. Ni, and T. L. Lee, "Implementation of a bidirectional three-phase dual-active-bridge dc converter with hybrid modulation for electric vehicle applications," Intelligent Green Building and Smart Grid (IGBSG), 2014 International Conference on, pp. 1–4, Apr. 2014.

[11] L. Tang, and G. J. Su, "Experimental investigation of a soft-switching three-phase, three-voltage bus dc/dc converter for fuel cell vehicle applications," IEEE Power Electronics Specialists Conference, pp. 585–591, June 2008.

[12] S. Baek, S. Dutta, and S. Bhattacharya, "Characterization of a three-phase dual active bridge dc/dc converter in wye-delta connection for a high frequency and high power applications," IEEE Energy Conversion Congress and Exposition, pp. 4183–4188, Sept. 2011.

[13] H. M. de O. Filho, D. S. Oliveira, C. E. de A. e Silva, and F. L. Tofoli, "Zvs bidirectional isolated three-phase dc-dc converter with dual phase-shift and variable duty cycle," Industry Applications (INDUSCON), 2012 10th IEEE/IAS International Conference on, pp. 1–8, Nov. 2012.

[14] J. Zhou, M. Xu, and F. C. Lee, "A novel current-tripler dc/dc converter," Power Electronics Specialist Conference, 2003. PESC'03. 2003 IEEE 34th Annual, vol. 3, pp. 1373–1378, IEEE, June 2003.

[15] M. Xu, J. Zhou, and F. C. Lee, "A current-tripler dc/dc converter," IEEE Transactions on Power Electronics, vol. 19, no. 3, pp. 693–700, May 2004.

[16] D. Liu, and H. Li, "A three-port three-phase dc-dc converter for hybrid low voltage fuel cell and ultracapacitor,"IECON 2006-32nd Annual Conference on IEEE Industrial Electronics, pp. 2558–2563, Nov. 2006.

[17] M. Kwon, J. Park, and S. Choi, "A bidirectional three-phase push-pull converter with dual asymmetrical pwm method," Future Energy Electronics Conference (IFEEC), 2013 1st International, pp. 161–167, Nov. 2013.

[18] G. Chen, Y. Lee, S. Y. R. Hui, D. Xu, and Y. Wang, "Actively clamped bidirectional flyback converter," IEEE Transactions on Industrial Electronics, vol. 47, no. 4, pp. 770–779, Aug. 2000.

[19] W. Li, H. Wu, H. Yu, and X. He, "Isolated winding-coupled bidirectional ZVS converter with PWM plus phase-shift (PPS) control strategy," IEEE Transactions on Power Electronics, vol. 26, no. 12, pp. 3560–3570, Dec. 2011.

[20] T. Bhattacharya, V. S. Giri, K. Mathew, and L. Umanand, "Multiphase Bidirectional Flyback Converter Topology for Hybrid Electric Vehicles," IEEE Transactions on Industrial Electronics, vol. 56, no. 1, pp. 78–84, Jan. 2009.

[21] F. Forest, B. Gelis, J. J. Huselstein, B. Cougo, E. Laboure, and T. Meynard, "Design of a 28 V-to-300 V/12 kW Multicell Interleaved Flyback Converter Using Intercell Transformers", IEEE Transactions on Power Electronics, vol. 25, no. 8, pp. 1966–1974, Aug. 2010.

[22] B. Tamyurek, and B. Kirimer, "An Interleaved High-Power Flyback Inverter for Photovoltaic Applications", IEEE Transactions on Power Electronics, vol. 30, no. 6, pp. 3228–3241, June 2015.

[23] M. B. El Kattel, R. Mayer, S. V. G. Oliveira, Y. R. de Novaes and A. Péres, "Three-phase flyback/current-fed push-pull dc-dc converter with y-Δ connected transformer," 2015 IEEE 13th Brazilian Power Electronics Conference and 1st Southern Power Electronics Conference (COBEP/SPEC), Fortaleza, 2015, pp. 1-6.

[24] M. Berrehil El Kattel, S. V. G. Oliveira, A. Pérez, R. Hausmann, A. Braatz and J. C. Dias, "Three-phase Flyback-Boost DC-DC converter with three-phase high frequency isolation," 2013 Brazilian Power Electronics Conference, Gramado, 2013, pp. 107-114.

[25] B. Tamyurek and B. Kirimer, "An interleaved flyback inverter for residential photovoltaic applications," Power Electronics and Applications (EPE), 2013 15th European Conference on, Lille, 2013, pp. 1-10

[26] J. Umuhoza, Y. Zhang, Y. Liu, J. Moquin, C. Farnell and H. A. Mantooth, "Interleaved Flyback based micro-inverter for residential photovoltaic application in remote areas," 2015 IEEE 16th Workshop on Control and Modeling for Power Electronics (COMPEL), Vancouver, BC, 2015, pp. 1-6.

[27] R. L. Andersen and I. Barbi, "A Three-Phase Current-Fed Push–Pull DC–DC Converter," in IEEE Transactions on Power Electronics, vol. 24, no. 2, pp. 358-368, Feb. 2009.

[28] S. V. G. Oliveira and I. Barbi, "A Three-Phase Step-Up DC–DC Converter With a Three-Phase High-Frequency Transformer for DC Renewable Power Source Applications," in IEEE Transactions on Industrial Electronics, vol. 58, no. 8, pp. 3567-3580, Aug. 2011.